

Experimental Study of Convective Heat Transfer and Thermal Performance in the Heat-Sink Channel with Various Geometrical Configurations Fins

¹Mohit Taneja, ²Sandeep Nandal, ³Arpan Manchanda, ⁴Ajay Kumar Agarwal

^{1,4}Asstt. Prof., Mechanical Engineering Department, R.I.M.T, Chidana, Sonipat, Haryana, India

²Asstt. Prof., Mechanical Engineering Department, DVCE Karnal, Haryana, India

³Asstt. Prof. & H.O.D, Mechanical Engineering Department, R.I.M.T, Chidana, Sonipat, Haryana, India

Abstract: An experimental study was conducted to investigate the heat transfer & friction loss characteristics in a heat sink channel with various geometrical configurations under constant heat flux conditions. The experiments are performed for the Reynolds number and heat flux in the ranges of 300 to 900 and 1.50-5.50kw/m², respectively. The heat sink with two different channel heights and two different channel widths are accomplished. Different geometrical configurations parameters effect of the micro-channel and heat flux on the heat transfer characteristics and pressure drop are considered. For those configurations the average heat transfer coefficient and Nusselt number were determined experimentally. The micro-channel geometry configuration has significant effect on the enhancement heat transfer and pressure drop. The results of this study are expected to lead to guidelines that will allow the design of the micro-channel heat exchangers with improved heat transfer performance of the electronic devices.

Keywords: Convective heat transfer, Heat sink, Experimental method, Air fluid flow, Heat transfer coefficient.

1. INTRODUCTION

The importance of heat transfer enhancement has gained greater significance in such areas as microelectronic cooling, especially in central processing units, macro and micro scale heat exchangers, gas turbine internal airfoil cooling, fuel elements of nuclear power plants, and bio medical devices. A tremendous amount of effort has been devoted to developing new methods to increase heat transfer from finned surface to the surrounding flowing fluid. At the conventional scale, heat sinks with various geometrical configurations have been used in various industries. However, the studies and applications on the micro-scale heat transfer devices are still limited. C.Y. Zhao et al. [1] presented the analytical and numerical study effect of porosity on the thermal performance a micro-channel heat sink. K.H. Ambatirudi et al. [2] Analyzed the heat transfer in micro-channel heat sinks. H. Honda et al. [3] reviewed the researches concerning the boiling heat transfer

enhancement for the micro-channel heat sink immersed in dielectric liquids. J. Luo [4] applied the theory of finite time thermodynamics to analyze and optimize the performance of a thermoelectric refrigerator. T.Q. Feng et al. [5] developed a three-dimensional analytical solution using the method of Fourier expansion for determination of the spreading thermal resistance of a cubic heat spreader for electronic cooling applications. H. Bhowmil [6] studied on the steady-state convective heat transfer of water from an in-line four electronic chips in a vertical rectangular channel. H.Y. Li et al. [7] determined the thermal performance of heat sinks with confined impingement cooling. X. Yu [8] studied on the thermal performance of a plate-pin fin heat sink and a plate fin heat sink. Y. Peles [9] experimentally studied on the single-phase heat transfer, boiling heat transfer and pressure drop of R-123 over a bank of shrouded micro-pin fins. K. Yakut [10] considered effects of the heights, widths of the hexagonal fins on thermal resistance and pressure drop characteristics. K.S. Yang et al. [11] experimentally studied on the heat transfer coefficient of pin fin heat sinks with different cross sections. C. Hong et al. [12] studied on the heat transfer characteristics of gaseous flows in a micro-channel and a microtube. T.M. Jeng et al. [13] experimentally studied the pressure drop and heat transfer of a square pin-fin array in a rectangular channel. As mentioned above, the numerous works have been reported concerning the heat transfer and pressure drop in the heat sink with various geometrical configurations, however, there still remains room to discuss on the heat transfer characteristics and pressure drop in the micro-channel heat sink. In the present paper, the main concern is to analysis of convective heat transfer characteristics and pressure drop in the various geometrical configurations heat sinks. Effects of various relevant parameters on the heat transfer and pressure drop characteristics are also considered.

2. EXPERIMENTAL SETUP AND PROCEDURE

2.1 Test rig

Fig. 1 shows a schematic diagram of the experimental system for the flow friction and heat transfer measurements for the heat sink. The experimental setup consists of a test section, air loop and data acquisition system. The wind tunnel, having dimensions 5*5cm and the length of 150cm. The air is drawn into the wind tunnel by the blower and is passed through a

mixing device. After that, the air enters in a straightener, test section and then discharged to the atmosphere. The air mass flow rate is measured by the nozzle flow meter. The pressure drops across the test section are measured by the differential pressure transducer. There are four pressure taps on each wall upstream and downstream of the test section. The type-T thermocouples with an accuracy of 0.1% of full scale are employed to measure air temperatures. The inlet and outlet temperatures of air are measured by two and four thermocouples with 1 mm diameter probes extending into the duct in which the air flows, respectively. All the thermocouples probes are pre-calibrated by dry-box temperature calibrator with 0.01 °C precision.

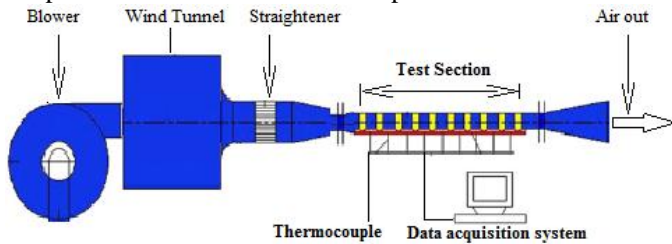


Fig1. Schematic diagram of experimental apparatus.

2.2 Test Section

Fig. 2 shows the schematic diagram of the test section. The width and length of the test section are 30 and 45mm, respectively. The heat sinks channels are accomplished by the wire electrical discharge machine. The details of the channel are listed in Table 1. An AC power supply is the source of power for the plate type heaters. Rear face of the test section is insulated with a 12mm thick heat resistant Mica standard sheet, 6 mm thick Aeroflex standard sheet, and then 5mmthickAcrylic standard sheet, respectively. Two type-T copper– constantan thermocouples with 1 mm diameter probes are used to measure the heat sink wall temperature. The thermocouple was installed by mounting on the wall (drilled holes from the rear face) and fixed at the rear face of the wall.

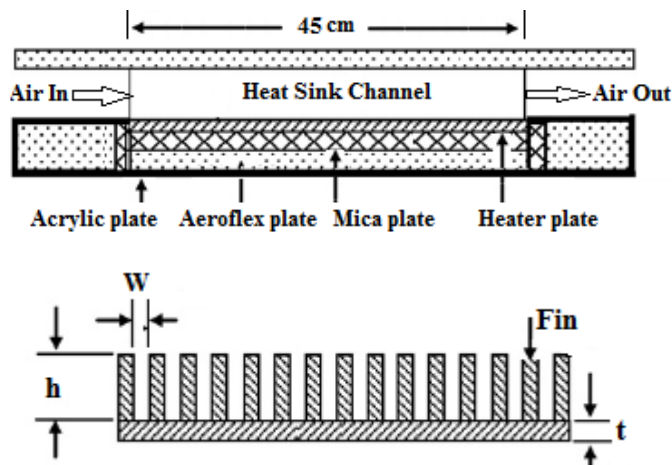


Fig.2. Schematic diagram of the test section & heat sink.

2.3. Operating conditions

Experiments were conducted with various heat flux and flow rates of air entering the test section. In the experiments, air flow rate was increased in small increments while the supplied heat at the micro-channel heat sink was kept constant. The supplied heat into the heat sink channel walls was adjusted to achieve the desired level by using electric heaters. The supplied power was calculated using the measured voltage and current supplied to the heaters. The supplied voltage and current to the heaters were measured by the digital meter. The steady-state sensible heat gain by the air flow can be determined from an energy balance. The average heat transfer, Q_{av} , is averaged from the supplied heat transfer to the heater and the removal heat transfer by cooling air. The temperature at each position and pressure drop across the test section were recorded three times. The temperatures of the inlet air into the test section and into the straightener were also checked. After as elapsed time of roughly 1-hours, the temperature of the heater plate reached steady state. The temperatures of the heat sink channel were measured by using calibrated copper-constantan thermocouples.

Table 1: Dimensions of the heat sink channel

Channel	Channel height, h (mm)	Fin & base thickness, t (mm)	Channel width, w (mm)	Size of heat sink (mm)
1	1.50	0.30	0.30	45*30
2	1.50	0.30	0.40	45*30
3	2.00	0.30	0.30	45*30
4	2.00	0.30	0.40	45*30

3. DATA REDUCTION

The data reduction of the measured data is summarized in the following procedures:

Heat transferred to the cooling air in the test section, Q_a , can be calculated from

$$Q_a = m_a C_p (T_o - T_{in}) \tag{1}$$

Where m_a is the air mass flow rate, C_p , is the specific heat of air, T_{in} and

T_{out} are the average inlet and outlet air temperatures, respectively.

Heat added to the micro-channel heat sink can be calculated from measuring voltage and current supplied the test section as follows:

$$Q_{heater} = V.I \tag{2}$$

The average heat transfer rate, Q_{av} , used in the calculation is determined from the heat removal my cooling air and the heat supplied to the heat sink as follows:

$$Q_{av} = \frac{Q_a + Q_{heater}}{2} \tag{3}$$

The average heat transfer coefficient of the micro-channel heat sink, h_m , can be calculated from the average heat transfer rate obtained from:

$$Q_{av} = h_m A_m (\Delta T_{LMTD}) \quad (4)$$

$$\Delta T_{LMTD} = \frac{(T_s - T_{a,in}) - (T_s - T_{a,out})}{\ln \left(\frac{T_s - T_{a,in}}{T_s - T_{a,out}} \right)} \quad (5)$$

Where T_s is the average surface temperature and A_m is the surface area of the micro-channel heat sink.

The average heat transfer coefficient is presented in terms of average Nusselt number as follows:

$$Nu = \frac{h_m D_h}{k} \quad (6)$$

Where k is the thermal conductivity of air, D_h is the hydraulic diameter of the channel before entering the test section.

Reynolds number based on the hydraulic diameter, D_h , of the channel as follows:

$$Re = \frac{u \cdot D_h}{\nu} \quad (7)$$

$$D_h = \frac{4 \cdot a}{P} \quad (8)$$

Where u is the air velocity, ν is the viscous of air, a is the cross section area of the channel before entering the test section, and P is the wet perimeter of the channel.

Thermal performance factor can be calculated by using the average Nusselt number ratio and the friction factor ratio as follows:

$$TP = \left(\frac{Nu}{Nu_o} \right) \left(\frac{f}{f_o} \right)^{-1/3} \quad (9)$$

4. RESULT AND DISCUSSION

Fig. 3 shows the variation of the outlet air temperature with air Reynolds number for different channel widths. Higher heat transfer rate as air mass flow rate increases. However, increase of heat transfer rate is less than that of air mass flow rate. Therefore, outlet air temperature tends to decrease as air mass flow rate increases. Higher surface area and surface roughness result in increase heat transfer rate, therefore, the outlet air temperatures of channel with of $w=0.3$ mm are higher than those of $w=0.4$ mm.

Fig. 4 shows the variation of the average heat sink temperature with air Reynolds number for different channel widths and different channel heights. As expected, the heat transfer rate depends on the cooling capacity rate of air. Therefore, the average heat sink temperature decreases as air Reynolds number increases. As seen in Fig. 3, due to the higher surface heat transfer area, the lower channel width heat sink gives average heat sink temperature lower than that higher one. However, this parameter has slightly effect on average heat sink temperature. The reason for this is that the micro-channel widths are close in the present study. In addition, average heat sink temperatures at higher channel height are lower than those from lower ones.

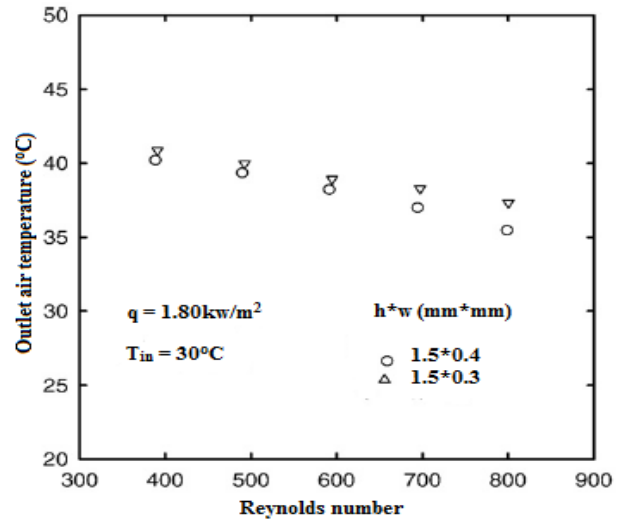


Fig.3. Variation of outlet air temperature with air Reynolds number for different channel width.

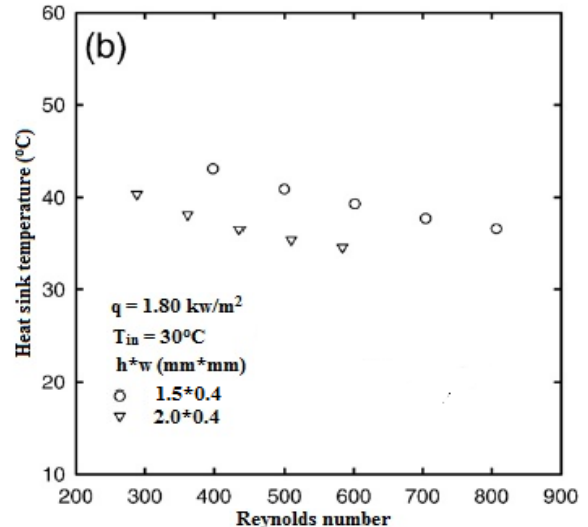
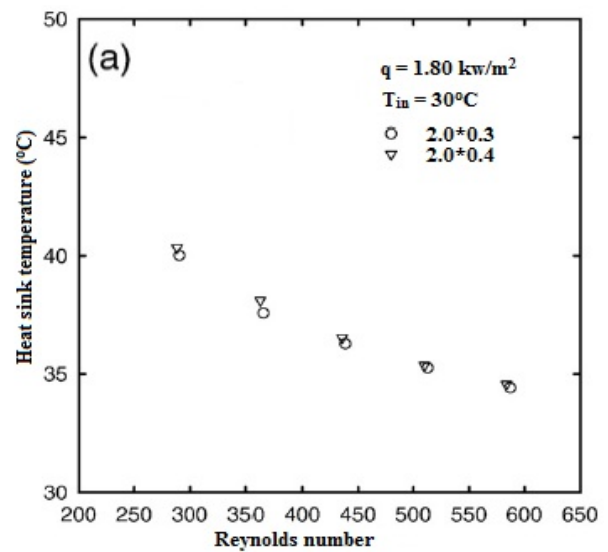


Fig.4 Variation of heat sink temperature with air Reynolds number for (a) different channel widths (b) different channel heights.

Due to higher surface area and surface roughness, the heat transfer rate from the heat sink surface to the cooling air increases.

Therefore, the increase channel height results in lower heat sink temperatures.

Fig. 5 shows the variation of the average heat transfer coefficient with air Reynolds number. As expected, the heat transfer coefficient increases with increasing heat flux. Due to higher temperature difference between inlet air temperature and heat sink temperature, higher heat flux gives heat transfer coefficient higher than those lower ones. Fig. 5 also shows the variation of the average heat transfer coefficient calculated from the present experiment with air Reynolds number of various geometrical configurations. It can be clearly seen from both figures that the heat transfer coefficients significant increase with increasing air Reynolds number. This is because the heat transfer coefficient depends on the heat transfer rate. For a given air Reynolds number, the heat transfer coefficients at $w=0.3$ mm are higher than those of $w=0.4$ mm as shown in Fig. 5(b).

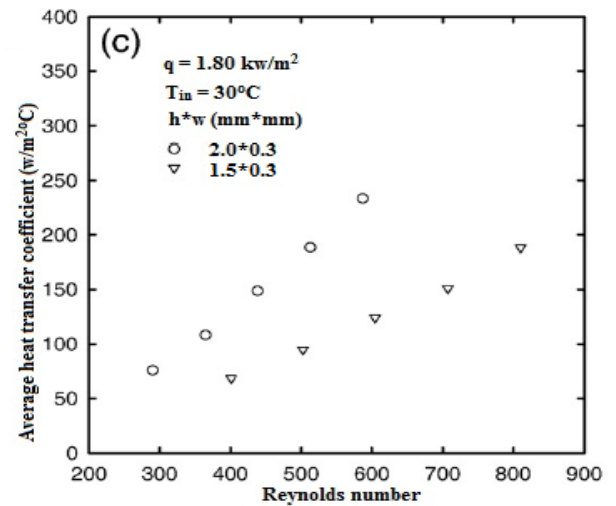
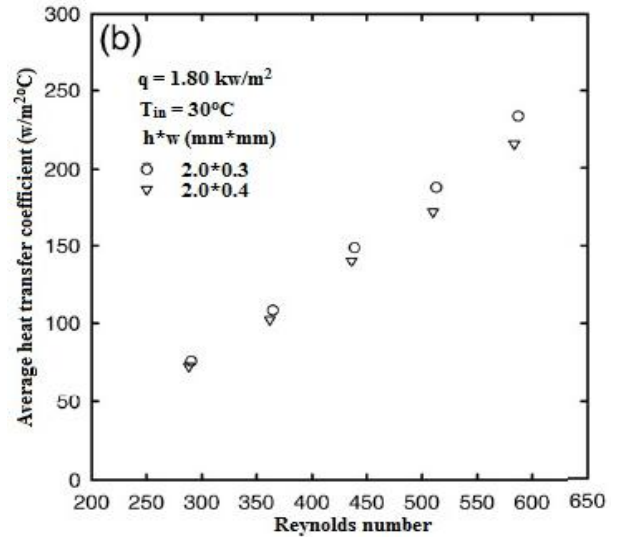
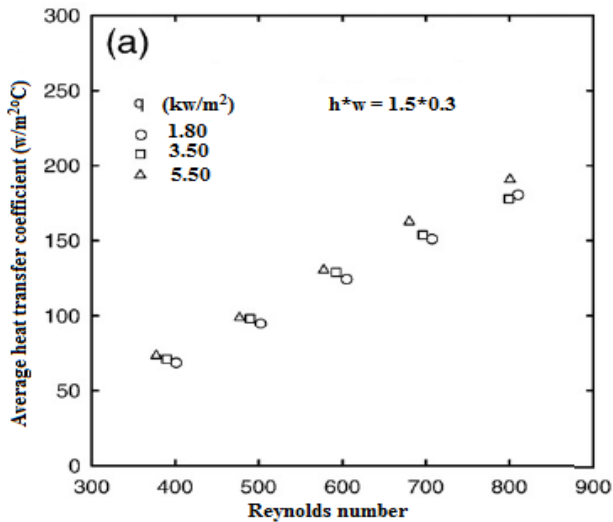


Fig. 5. Variation of average heat transfer coefficient with air Reynolds number for (a) different heat fluxes (b) different channel widths (c) different channel heights.

Effect of channel height on the enhancement of average heat transfer coefficient is shown in Fig. 6(c). Due to higher heat transfer area and higher surface roughness, the average heat transfer coefficients of the heat sink with $h=2.0$ mm are higher than those with $h=1.5$ mm. In addition, the results can be shown in another form as shown in Fig. 6 and the same explanation as for Fig. 5 can be given.

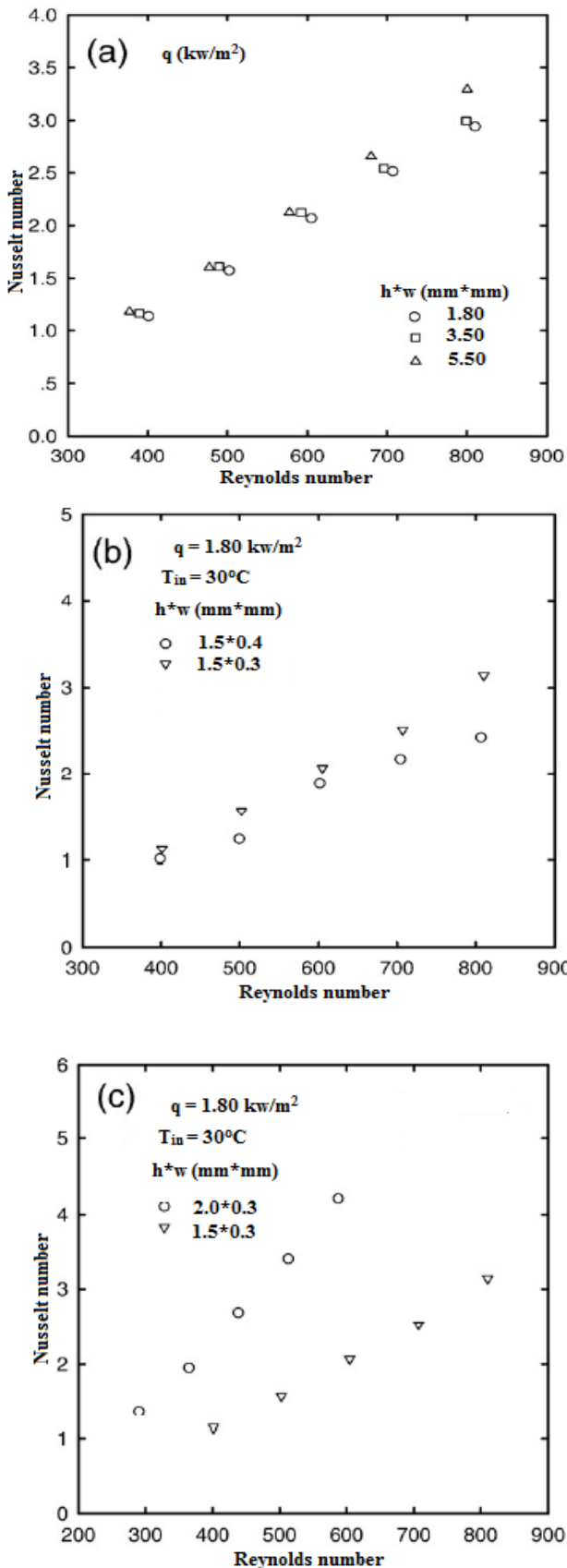


Fig. 6. Variation of Nusselt number with air Reynolds number for (a) different heat fluxes (b) different channel widths (c) different channel heights.

Fig. 7 shows the variation of pressure drop per unit length for different geometrical configurations. Due to the higher surface force and higher surface roughness, the flow characteristics through the micro-channel is quite high and complex as compare to the conventional scale. Usually, the surface roughness is represented in terms of the average surface roughness. For the conventional tubes, the roughness can be obtained from tables given by Moody [46] according to the tube machining techniques and materials. For the micro-scale, however, these values still require to be verified.

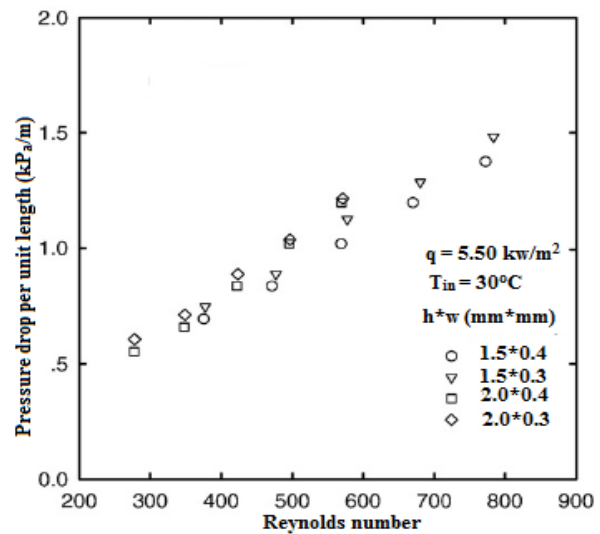


Fig. 7. Variation of pressure drop with air Reynolds number for different channel geometrical configurations.

It can be clearly seen from the figure that the pressure drop continues to increase with Reynolds number. In addition, the shape and the size of roughness irregularities of the micro-channel surface have significant effect on the pressure drop variations as shown in Fig. 7.

5. CONCLUSIONS

With the research and development of the electronics products & devices & their technologies, mini and micro-channel cooling systems have been widely used in the electronic circuits. However, the friction factor and heat transfer performance for the micro-channel are still to be legally valid. The heat transfer characteristics and pressure drop in the micro-channel heat sinks with various geometrical configurations are tested experimentally. It is found that the shape and the size of roughness factor of the micro-channel surface have a large scale effect on enhancement of heat transfer performance and the pressure drop variations.

REFERENCES

1. C.Y. Zhao, T.J. Lu, Analysis of microchannel heat sink for electronics cooling, *International Journal of Heat and Mass Transfer* 45 (2002) 4857–4869.
2. K.H. Ambatirudi, M.M. Rahman, Analysis of conjugate heat transfer in microchannel heat sinks, *Numerical Heat Transfer* 37 (2000) 711–731.
3. J.J. Wei, H. Honda, Effects of fin geometry on boiling heat transfer from silicon chips with micro-pin-fins immersed in FC-72, *International Journal of Heat and Mass Transfer* 46 (2003) 4059–4070.
4. J. Luo, Optimum allocation of heat transfer surface area for cooling load and COP optimization of a thermoelectric refrigerator, *Energy Conservation and Management* 44 (2003) 3197–3206.
5. T.Q. Feng, J.L. Xu, An analytical solution of thermal resistance of cubic heat spreaders of electronic cooling, *Applied Thermal Engineering* 24 (2004) 323–337.
6. H. Bhowmil, Convection heat transfer from discrete heat sourced in a liquid cooled rectangular channel, *Applied Thermal Engineering* 25 (2005) 2532–2542.
7. H.Y. Li, S.M. Chao, G.L. Tsai, Thermal performance measurement of Heat sinks with confined impinging jet by infrared thermography, *International Journal of Heat and Mass Transfer* 48 (2005) 5386–5394.
8. X. Yu, Development of a plate-pin fin heat sink and its performance comparisons with a plate fin heat sink, *Applied Thermal Engineering* 25 (2005) 173–182.
9. Y. Peles, Forced convective heat transfer across a pin fin micro heat sink, *International Journal of Heat and Mass Transfer* 48 (2005) 3615–3627.
10. K. Yukut, Experimental investigation of thermal resistance of a heat sink with hexagonal fins, *Applied Thermal Engineering* 26 (2006) 2262–2271.
11. K.S. Yang, W.H. Chu, I.Y. Chen, C.C. Wang, A comparative study of the airside performance of heat sinks having pin fin configurations, *International Journal of Heat and Mass Transfer* 50 (2007) 4607–4613.
12. C. Hong, Y. Asako, Heat transfer characteristics of gaseous flows in a microchannel and a microtube with constant wall temperature, *Numerical Heat Transfer* 52 (2007) 219–238.
13. T.M. Jeng, S.C. Tzeng, Pressure drop and heat transfer of square pin-fin arrays in inline and staggered arrangements, *International Journal of Heat and Mass Transfer* 50 (2007) 2364–2375.
14. L.F. Moody, Friction factors for pipe flow, *Trans. ASME* 66 (1944) 671–683.
15. Frank M. White, *Viscous Fluid Flow*. McGraw-Hill, New York, 1991.
16. W.M. Kays and M.E. Crawford, *Convective Heat and Mass Transfer* (2nd Edn.), McGraw-Hill Book Co., New York, U.S.A. (1980).